Actions of noradrenaline on substantia gelatinosa neurones in the rat spinal cord revealed by *in vivo* patch recording

Motoki Sonohata[1,2], Hidemasa Furue[1], Toshihiko Katafuchi[1], Toshiharu Yasaka[1], Atsushi Doi[1], Eiichi Kumamoto[2] and Megumu Yoshimura[1]

[1] *Department of Integrative Physiology, Graduate School of Medical Sciences, Kyushu University, Fukuoka 812-8582, Japan*
[2] *Department of Physiology, Saga Medical School, Saga 849-8501, Japan*

To elucidate the mechanisms of antinociception mediated by the descending noradrenergic pathway in the spinal cord, the effects of noradrenaline (NA) on noxious synaptic responses of substantia gelatinosa (SG) neurones, and postsynaptic actions of NA were investigated in rats using an *in vivo* whole-cell patch-clamp technique. Under urethane anaesthesia, the rat was fixed in a stereotaxic apparatus after the lumbar spinal cord was exposed. In the current-clamp mode, pinch stimuli applied to the ipsilateral hindlimb elicited a barrage of EPSPs, some of which initiated an action potential. Perfusion with NA onto the surface of the spinal cord hyperpolarized the membrane (5.0–9.5 mV) and suppressed the action potentials. In the voltage-clamp mode (V_H, -70 mV), the application of NA produced an outward current that was blocked by Cs^+ and GDP-β-S added to the pipette solution and reduced the amplitude of EPSCs evoked by noxious stimuli. Under the blockade of postsynaptic actions of NA, a reduction of the evoked and spontaneous EPSCs of SG neurones was still observed, thus suggesting both pre- and postsynaptic actions of NA. The NA-induced outward currents showed a clear dose dependency (EC_{50}, 20 μM), and the reversal potential was -88 mV. The outward current was mimicked by an α_2-adrenoceptor agonist, clonidine, and suppressed by an α_2-adrenoceptor antagonist, yohimbine, but not by α_1- and β-antagonists. These findings suggest that NA acts on presynaptic sites to reduce noxious stimuli-induced EPSCs, and on postsynaptic SG neurones to induce an outward current by G-protein-mediated activation of K^+ channels through α_2-adrenoceptors, thereby producing an antinociceptive effect.

Several lines of evidence indicate that noxious information is transmitted through the myelinated Aδ- and unmyelinated C-afferent fibres from the periphery to the superficial dorsal horn especially the substantia gelatinosa (SG) (lamina II of Rexed, 1952) neurones (Kumazawa & Perl, 1978; Sugiura *et al.* 1986; Yoshimura & Jessell, 1989). Catecholamines, such as adrenaline and noradrenaline (NA), modulate noxious transmission at several sites from the peripheral nerves to the central nervous system (CNS). For example, NA released from sympathetic nerve terminals produces hyperalgesia by acting on the dorsal root ganglion cells and the peripheral nerves under pathological conditions such as peripheral inflammation (Kasai & Mizumura, 2001) and nerve injury (McLachlan *et al.* 1993; Perl, 1999). On the other hand, adrenaline

has been used in spinal anaesthesia together with local anaesthetics for its vasoconstrictive effect to decrease clearance of the anaesthetics (Concepcion *et al.* 1984; Vaida *et al.* 1986) and for its direct actions within the spinal dorsal horn (Reddy *et al.* 1980; Howe *et al.* 1983; North & Yoshimura, 1984; Baba *et al.* 2000*a*,*b*). Behavioural studies have also shown that α_2-adrenoceptors mediate spinal analgesia and adrenergic-opioid synergy that may be useful in clinical pain management (Stone *et al.* 1997; Fairbanks *et al.* 2002).

The existence of dense NA-containing nerve terminals in the superficial lamina of the spinal dorsal horn has been demonstrated (Satoh *et al.* 1982; Hagihira *et al.* 1990; Rajaofetra *et al.* 1992). These fibres originate from the cell groups of A5, A6 (nucleus locus ceruleus) and

A7 (subceruleus) in the pons (Westlund *et al.* 1982), and are designated as the descending noradrenergic pain inhibitory pathway. In fact, behavioural studies have demonstrated that the intrathecal administration of NA has an antinociceptive effect when assessed by the tail-flick tests (Concepcion *et al.* 1984; Vaida *et al.* 1986). Recent anatomical studies have shown that α_{2C}-adrenergic receptors are localized on the axon terminals of excitatory interneurones in the superficial dorsal horn that are in contact with spinomedullary projecting neurones, thus possibly contributing to noradrenergic antinociception (Olave & Maxwell, 2003*a*,*b*). However, the cellular mechanisms of the inhibitory effects of NA on the noxious pain transmission are still not fully understood.

Electrophysiological studies have demonstrated that iontophoretic application of NA induces reduction of single unit responses to noxious stimuli in dorsal horn neurones of anaesthetized rats (Headley *et al.* 1978; Howe & Zieglgansberger, 1987). Intracellular (North & Yoshimura, 1984) and whole-cell patch-clamp (Yajiri *et al.* 1997; Baba *et al.* 2000*a*,*b*) recordings have revealed that NA produces hyperpolarization and an outward current, respectively, in a proportion of SG neurones in transverse spinal cord slices. In addition, NA has also been shown to suppress the dorsal root-evoked EPSCs in SG neurones through an action on primary afferent terminals *in vitro* (Kawasaki *et al.* 2003). However, it has not been determined whether the EPSCs that are inhibited by NA are responsible for pain transmission in slice preparations. In addition, the effects of NA on EPSCs have not yet been examined in either the intracellular or whole-cell patch-clamp recordings of *in vivo* animals. Furthermore, although some SG neurones have been shown to spread their dendrites more than 500 μm rostrocaudally (Spike & Todd, 1992), the thickness of the transverse spinal cord slices was usually less than 500 μm (Yoshimura & Jessell, 1989). Therefore, it is possible that the dendrites of the SG neurones are transected and/or injured in the slice preparations, thus making it difficult to evaluate the overall effect of NA on the SG neurones. We thus sought to investigate the effects of NA on synaptic responses to noxious stimuli and also analyse the postsynaptic actions of NA on SG neurones under *in vivo* conditions. For this purpose we used *in vivo* whole-cell patch-clamp technique in anaesthetized rats. We have recently established a technique for patch-clamp recordings from the rat spinal cord (Furue *et al.* 1999; Narikawa *et al.* 2000), although *in vivo* patch-clamp recordings have been reported so far in the rat cortex (Zang *et al.* 2003; Petersen *et al.* 2003). In the present study, we applied NA by perfusing it onto the surface of the spinal cord and were thus able to investigate the effects of NA on rat SG neurones pharmacologically using antagonists and agonists for adrenoceptor subtypes, which were analysed using an *in vivo* patch-clamp technique.

Methods

All the experimental procedures involving the use of animals were approved by the Ethics Committee on Animal Experiments, Kyushu University, and were in accordance with the UK Animals (Scientific Procedures) Act 1986 and associated guidelines.

Preparation

The methods used for the current experiment were modifications of those used in our preceding studies (Furue *et al.* 1999; Narikawa *et al.* 2000). Briefly, male Sprague–Dawley rats (6–8 weeks of age, 200–300 g) were anaesthetized with urethane (1.2–1.5 g kg^{-1}, intraperitoneal). In contrast to the previous studies, artificial ventilation and pneumothorax were not made. However the rats could be maintained in good condition without artificial ventilation by supplying oxygen through a nose cone. If a withdrawal reflex appeared, then a supplemental dose of urethane was given during surgery and the data collection period. The rectal temperature was kept at 37–38°C by a heating pad placed beneath the animal. The lumbar spinal cord was exposed at the level from L3 to L5 by a thoraco-lumbar laminectomy at the level from Th12 to L3, and then the rat was placed in a stereotaxic apparatus (Model ST-7, Narishige, Japan) (Fig. 1*A*). After opening the dura, a dorsal root that enters the spinal cord above the level of recording sites was lifted using a glass retractor, so that a recording electrode could be advanced into the SG from the surface of the spinal cord. The pia-arachnoid membrane was cut to make a window large enough to allow the patch electrode to enter the spinal cord (Fig. 1*B*). The surface of the spinal cord was irrigated with 95% O_2–5% CO_2-equilibrated Krebs solution (15 ml min^{-1}) (mM: NaCl 117, KCl 3.6, CaCl$_2$ 2.5, MgCl$_2$ 1.2, NaH$_2$PO$_4$ 1.2, glucose 11, and NaHCO$_3$ 25) through glass pipettes at 36.5 $\pm$ 0.5°C (Fig. 1*A*). At the end of the experiments the rats were given an overdose of urethane and were then killed by exsanguination.
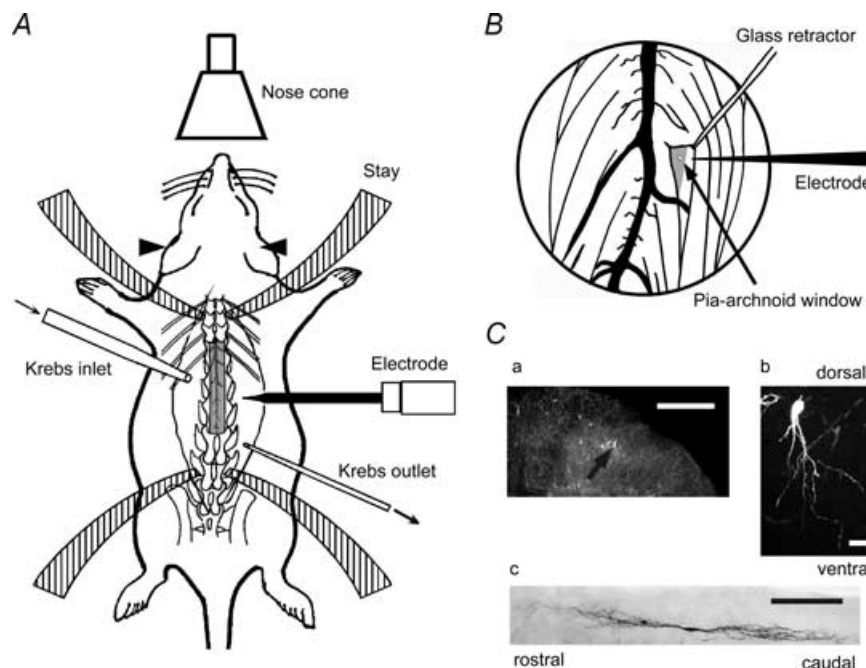
Patch-clamp recordings

The patch electrodes were pulled from thin-walled borosilicate glass capillaries (o.d. 1.5 mm) using a puller (p-97, Sutter Instrument, USA), and were filled with a

patch-pipette solution composed of the following (mM): potassium gluconate 135 or caesium sulphate 110, KCl 5, CaCl$_2$ 0.5, MgCl$_2$ 2, EGTA 5, ATP-Mg 5, Hepes-KOH 5; pH 7.2. When necessary, guanosine-5′-O-(2-thiodiphosphate) (GDP-β-S) was added at a concentration of 2 mM to the patch-pipette solution. The electrode with a resistance of 5–12 MΩ was advanced at an angle of 30–45 deg into the SG through the window using a micromanipulator (Model WR-88, Narishige, Japan). After making a gigaohm seal (resistance of at least 10 GΩ), the membrane patch was ruptured by a brief period of more negative pressure, thus resulting in the whole cell configuration. Recordings were made using a patch-clamp amplifier (Axopatch 200B, Axon Instruments, Union City, CA, USA), and the data were digitized with an A/D converter (Digidata 1200, Axon Instruments), stored on a personal computer using a data acquisition program (pCLAMP 7, Axon Instruments), and then analysed using a software package (AxoGraph 4.6, Axon Instruments). To examine changes in the membrane conductance of the NA-induced currents, 10 mV voltage steps (duration: 200 ms)

from a holding potential (V_{H}) of –70 mV to voltages ranging from −60 to 20 mV were given to the SG neurones in the absence and presence of NA.

Cell identification

Neurones were recorded at a depth of 50–150 μm measured from the dorsal surface of the spinal cord to the point of contact with the cell. This distance was identified to be within the SG using transverse slices obtained from the spinal cords of 6- to 8-week-old rats at the same lumbar level (Furue *et al.* 1999). The location and morphological features of the recorded cells were further confirmed in some instances by an intrasomatic injection of neurobiotin (0.2% in electrode solution). After terminating the electrophysiological recordings, the rats were deeply anaesthetized with supplemental urethane and perfused transcardially with 4% paraformaldehyde in 0.1 M phosphate buffer (PB, pH 7.4). The spinal cords were removed and immersed overnight in the same fixative at 4°C and rinsed in 0.1 M PB. The

Figure 1. Schematic diagrams of *in vivo* rat preparation and identification of SG neurones from which whole-cell patch-clamp recordings were taken

A, while supplying oxygen to a urethane-anaesthetized rat from a nose cone, the lumbar spinal cord at the level from L3 to L5 was exposed by laminectomy. Arrowheads indicate ear bar. Stay was a part of the stereotaxic apparatus to fix the spine. *B*, magnified view of the spinal cord in which dorsal roots were lifted using a glass retractor. The superficial dorsal grey matter lateral to the dorsal root entry zone was discernible as a relatively translucent band under Lissauer's tract (grey zone). The pia-arachnoid membrane was cut to make a window to penetrate the patch electrode in the spinal cord. *Ca*, a recorded neurone identified with an intracellular injection with neurobiotin (fluorescence). *Cb* and *c*, morphological features in transverse (*b*; fluorescence) and sagital (*c*; DAB) planes. Scale bars in *Ca*, *b* and *c* are 200, 20 and 200 μm, respectively.

spinal cord segments were sectioned transversely into 100 μm-thick slices using a Vibratome. To examine the expansion of dendrites of the recorded neurones, the parasagital sections with the same thickness were made in some instances. Visualization of neurobiotin-labelled cells was performed by diaminobenzidine (DAB)-based or fluorescence histochemistry. For DAB-based histochemistry free-floating sections were incubated in Vectastain (Elite kit; Vector Laboratories, Burlingame, CA, USA) according to the manufacturer's protocol. The peroxidase activity was revealed with DAB in the presence of hydrogen peroxide, and sections were mounted on gelatinized slides. Fluorescence histochemistry was performed as follows: free-floating sections were incubated overnight at 4°C in phosphate buffered saline (PBS) with 0.3% Triton X-100 containing streptavidine–Texas Red (diluted 1 : 1000), washed several times in PBS, and then coverslipped with Vectashield (Vector). The sections were viewed and photographed with a microscope (Olympus, Tokyo, Japan) or an LSM 510 laser scanning confocal microscope (Carl Zeiss, Oberkochen, German).

Pinch stimulation and drug application

The noxious mechanical stimuli were applied to the receptive field of the ipsilateral hindlimb with toothed forceps. To confirm that the responses were selectively activated by nociceptors, the toothed forceps was fixed on a rod and various weights were put on the forceps. The frequency of EPSCs increased as the weight increased and no significant accommodation was observed, thus indicating that the responses were mediated by the activation of nociceptors. Drugs dissolved in Krebs solution were applied to the surface of the spinal cord by exchanging solutions *via* three-way stopcocks without any change in either the perfusion rate or the temperature. The time necessary for the solution to flow from the stopcock to the surface of the spinal cord was approximately 5 s. The drugs used were NA (WAKO, Osaka, Japan), tetrodotoxin (TTX) (WAKO), GDP-β-S (Sigma, St Louis, MO, USA), prazosin (Sigma), clonidine (Sigma), phenylephrine (Sigma), isoproterenol (Sigma), yohimbine (WAKO), and propranolol (Sigma).

Statistical analysis

All numerical data were expressed as the mean ± S.E.M. Statistical significance was determined as $P < 0.05$ using ANOVA followed by Scheffe's test and indicated by asterisks in the figures. Correlations were analysed by Pearson's product moment test. In all cases, *n* refers to the number of neurones studied. The continuous theoretical curve for the concentration–response relationship of NA was drawn according to a modification of the Michaelis–Menten equation, $I = I_{max}C^n/(C^n + EC_{50}{}^n)$, using a least-square fitting routine (Newton–Raphson method) after normalizing the amplitude of the response, where I is the normalized value of the currents, I_{max} the maximal response, C the drug concentration, and n the apparent Hill coefficient. The membrane potentials were not corrected for the liquid junction potential between the Krebs and patch-pipette solutions.

Results

An animal preparation could be maintained in a stable condition for over 10 h, which was comparable to the previous experimental state using an artificial ventilator (Furue *et al.* 1999). Whole-cell patch-clamp recordings were made from 129 SG neurones. Stable recording was obtained from a single neurone for up to 5 h. All neurones studied had membrane potentials more negative than −55 mV. The membrane potentials were −64.2 ± 0.7 mV (*n* = 80), and the input membrane resistances were 311.7 ± 27.1 MΩ (*n* = 42). These values were almost the same as those reported previously (Furue *et al.* 1999). Under voltage-clamp conditions at a V_H of −70 mV, all SG neurones exhibited EPSCs with an average amplitude of 24.6 ± 2.1 pA (*n* = 11) and a frequency of 20.8 ± 3.5 Hz (*n* = 11).

The neurone shown in Fig. 1*Ca* was located in SG and possessed the morphological features of a rounded soma with dendrites branching off ventrally (Fig. 1*Cb*), similar to the cells previously described as SG neurones using either Golgi staining (Beal & Bicknell, 1985) or horseradish peroxidase labelling (Woolf & Fitzgerald, 1983). In some SG neurones the dendrites extended rostrocaudally over 800 μm in the parasagital section (Fig. 1*Cc*).

Effects of NA on the responses to noxious stimuli

In the current-clamp mode, pinch stimuli were applied to the receptive field of the ipsilateral hindlimb. As shown in Fig. 2*A*, left, pinch stimuli elicited a barrage of EPSPs, about half of which were accompanied by an action potential. The evoked EPSPs disappeared within 1 s after the stimulation, and did not show any desensitization of the responses. Perfusion with NA (50 μM) caused a slight hyperpolarization (5.0–9.5 mV) of the membrane potential and suppressed action potentials without affecting the increased number of EPSPs in a reversible manner (Fig. 2*A*, middle and right). The

NA-induced hyperpolarization and suppression of action potentials were observed in all five of the neurones tested. In the voltage-clamp mode ($V_H = -70$ mV), the pinch stimuli produced large and summated EPSCs at the beginning of the stimuli that were followed by a barrage of EPSCs, and again large EPSCs at the end of the stimuli (Fig. 2B, left). When NA was applied to the surface of the spinal cord, the amplitude of the evoked EPSCs decreased, although the amplitude of the large EPSCs at the beginning and end of stimulation was not affected (Fig. 2B, middle). The barrage of EPSCs induced by pinch again appeared after the washing-out of NA (right).

Characteristics of postsynaptic actions of NA

In the current-clamp mode, the perfusion of NA (50 μM) induced the hyperpolarization of the membrane potentials (6.6 ± 0.8 mV, $n = 5$) in all of eight SG neurones tested in a reversible manner. The hyperpolarization showed a gradual onset and recovery following the application of NA (Fig. 3A). In the voltage-clamp mode ($V_H = -70$ mV), 63 out of 74 SG neurones (85%) exhibited NA-induced outward currents (26.9 ± 2.6 pA) accompanied by a decrease in the frequency and mean amplitude of EPSCs (65.5 ± 10.8% of the control frequency, 83.0 ± 2.7% of control amplitude, $n = 6$) (Fig. 3B). The inset shows the EPSCs before (a) and during (b) the application of NA on an expanded time scale showing a smooth rising phase and long duration (~20 ms). In two neurones, the inward currents were observed (data not shown). When NA was administered 5 min after the first application, the response was again induced with almost the same amplitude (data not shown). Furthermore, the outward

currents did not show any accommodation during the continuous application of NA (50 μM) for more than 5 min, and they were also accompanied by a decrease in the amplitude of the EPSCs (Fig. 3C). The frequency and amplitude of EPSPs were suppressed by the application of TTX (1 μM) (51.7 ± 18.8% of control frequency, 83.0 ± 6.2% of control amplitude; $n = 5$) within 30 s (Fig. 3D), thus suggesting that a substantial amount of spontaneous EPSCs (sEPSCs) initiated by action potentials from interneurones or primary afferents were included under the *in vivo* condition in the present study. During the simultaneous application of TTX, NA (50 μM) also induced outward currents, but did not significantly affect the frequency and the amplitude of miniature EPSCs (mEPSCs) (see Kawasaki *et al.* 2003) (Fig. 3D).

Validity of drug application under *in vivo* conditions

In the present study, NA was perfused to the surface of the spinal cord. To evaluate the validity of the drug application, three parameters, namely the depth from the dorsal surface of the spinal cord to the point of contact with the cell, the amplitude and time from onset to peak of the outward currents, were measured in the NA (50 μM)-induced outward current (Fig. 4A). As shown in Fig. 4B and C, there was no correlation between the amplitude and depth (B, $r = -0.21$, $P > 0.05$, $n = 69$), and onset to peak and depth (C, $r = -0.074$, $P > 0.05$, $n = 63$). In our previous study, mechanical stimuli-induced EPSCs and inhibitory postsynaptic currents (IPSCs) in SG neurones were substantially suppressed by a non-*N*-methyl-D-aspartate (NMDA) receptor antagonist (Furue *et al.* 1999),
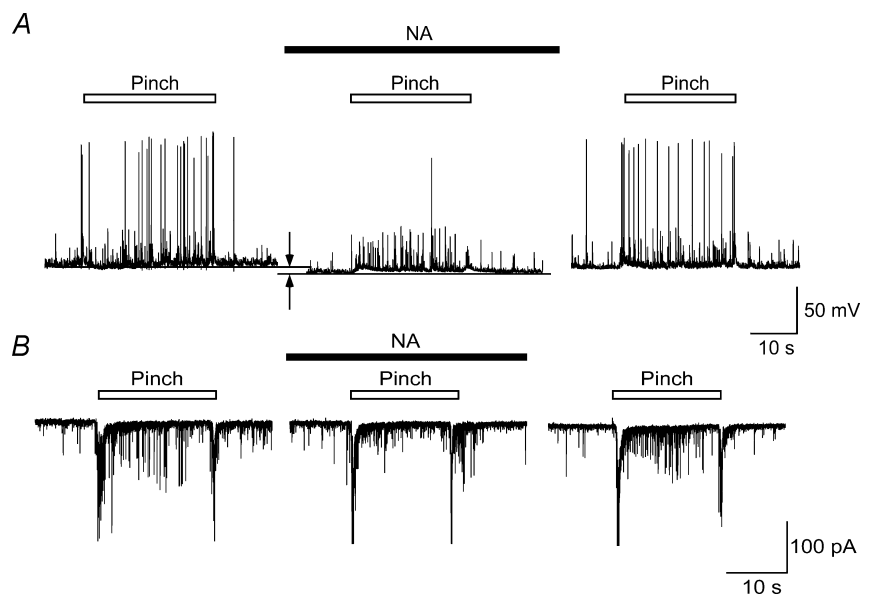
**Figure 2. Reduction of pinch-evoked firing of SG neurons by NA**

A, pinch stimuli applied to the ipsilateral hindlimb produced a barrage of EPSPs accompanied by action potentials under a current-clamp condition (left). NA (50 μM) hyperpolarized SG neurone (arrows) and inhibited the action potentials in a reversible manner (middle and left). *B*, left, EPSCs elicited by pinching in voltage-clamp mode ($V_H = -70$ mV). NA (50 μM) suppressed repeated EPSCs during pinching in a reversible manner without affecting amplitude of large EPSCs evoked at the beginning and end of pinch stimulus (middle and right).

and GABA and glycine antagonists (Narikawa *et al.* 2000), respectively, that were applied in the same manner as in the present study. In addition, the responses including post- and presynaptic actions were observed within 10 s after changing, by three-way stopcocks, from Krebs solution to a drug-containing solution. Furthermore, perfusion with NA (50 μM) to the spinal cord did not alter the blood pressure and heart rate (data not shown). These findings, taken together, suggest that the perfused drugs equally reach the recorded cells in the SG at a depth of 50–150 μm,

thereby inducing neuronal responses through a direct but not a systemic action.

Pharmacological analysis of the NA-induced responses

As shown in Fig. 5A, outward currents exhibited a clear dose dependency on NA perfused at the surface of the
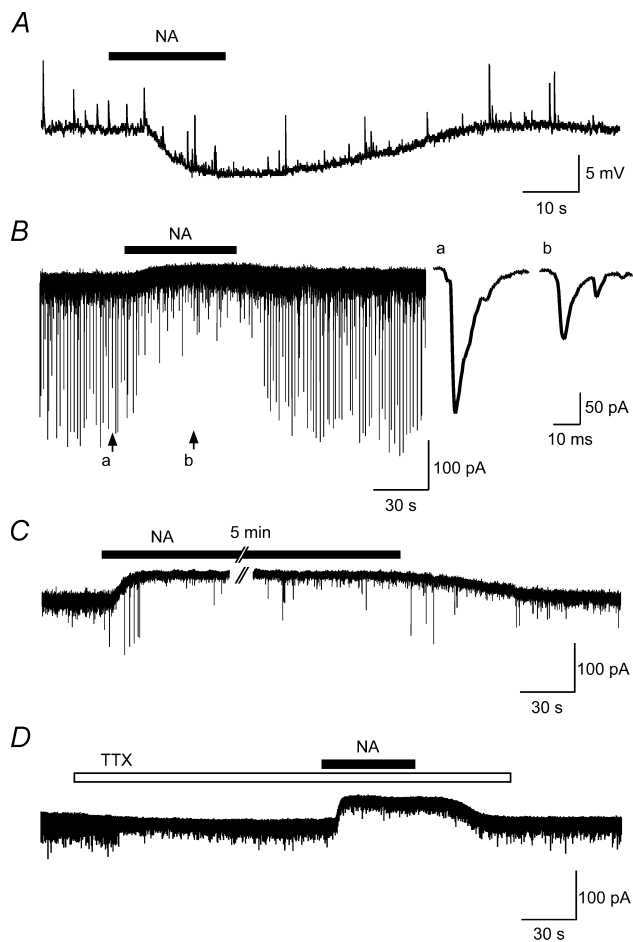
Figure 3. Characteristics of membrane responses induced by NA in SG neurones

A, NA (50 μM)-induced hyperpolarization in current-clamp mode. Resting membrane potential was −62.5 mV. *B*, in voltage-clamp mode (V_H = −70 mV), NA produced an outward current associated with a marked reduction of amplitude of sEPSCs. Inset, EPSCs before (*a*) and during (*b*) NA application in an expanded time scale. *C*, NA application for more than 5 min induced an outward current without desensitization. Note that amplitude of EPSCs decreased during NA application. *D*, tetrodotoxin (TTX, 1 μM) inhibited spontaneous excitatory postsynaptic currents (sEPSCs) shown by sudden decrease in amplitude of EPSCs within 1min after TTX. Under TTX, NA (50 μM) also produced an outward current without any decrease in amplitude of mEPSCs.
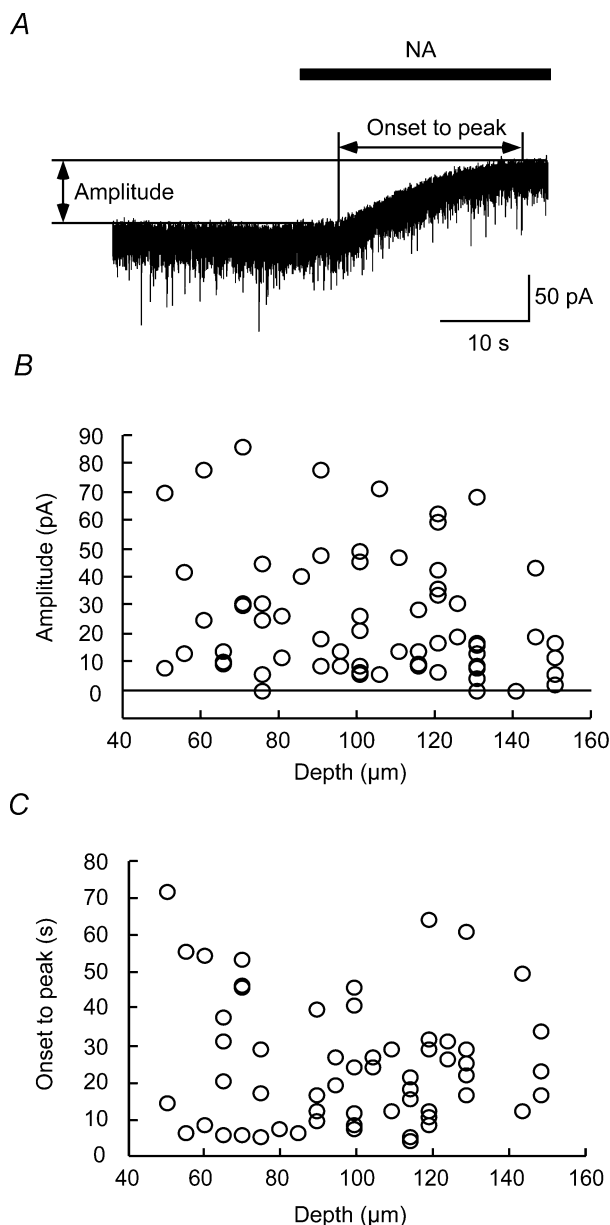
Figure 4. Correlation between amplitude or onset to peak of NA-induced currents and depth of recorded neurones

A, method for measuring amplitude and time from onset to the peak of outward current. *B*, no correlation between amplitude and depth of recorded neurones (*r* = −0.21, *P* > 0.05, *n* = 69). *C*, no correlation between onset to peak and depth (*r* = −0.07, *P* > 0.05, *n* = 63).

spinal cord. The onset of the responses became rapid and a recovery was delayed with an increasing concentration of NA. Figure 5*B* shows a dose–response curve of the NA-induced outward currents. An analysis of the curve based on the Hill plot gave 20.5 μM for a value of the effective concentration producing half-maximal response (EC$_{50}$) with a Hill coefficient of 1.39.

Figure 6*A* shows the NA (50 μM)-induced currents recorded at the different V_H values. When the amplitudes of the NA-induced currents were plotted against V_H, the reversal potential was −84 mV (Fig. 6*B*). Figure 6*C* demonstrates the relationships between the step voltage and steady current at the end of the pulses that were obtained in the absence (filled circles) and presence (open circles) of NA (50 μM). The net NA-induced current (filled triangles), calculated from the difference between the two currents, exhibited a reversal potential of −87.9 ± 3.3 mV ($n = 7$). The equilibrium potential (−92 mV) of K$^+$, as calculated from the Nernst equation using K$^+$ concentrations ([K$^+$]$_o$, 3.6 and [K$^+$]$_i$, 140 mM) of the solutions, was slightly different from the reversal potentials obtained from the patch-clamp experiment. This difference might be regarded as a liquid junction potential existing between the Krebs and patch-pipette solutions (Yajiri *et al.* 1997).

The NA (50 μM)-induced outward currents recorded with the pipette solution containing Cs$^+$ just after establishing the whole cell configuration (Fig. 7*A*, left) were abolished at the second application of NA, which was performed more than 5 min later (Fig. 7*A*, right, $n =$

6). To examine the involvement of G-proteins in the NA-induced outward current, GDP-β-S, a non-hydrolysable analogue of GDP that competitively inhibits G-proteins, was used. When NA (50 μM) was applied shortly after establishing the whole-cell configuration with pipettes containing potassium gluconate and GDP-β-S (2 mM), an outward current was observed although it was small in amplitude (Fig. 7*B*, left). Then the outward current was completely abolished when NA was again applied 10 min later (Fig. 7*B*, right, $n = 5$). These findings suggested that the NA-induced outward current was mediated by K$^+$ channels through an activation of G-proteins.

As shown in Fig. 8*A*, the NA (50 μM)-induced outward current as well as a slight decrease in EPSCs were attenuated by the application of an α_2-adrenoceptor antagonist, yohimbine (4 μM, $n = 6$), while an α_1-receptor antagonist, prazosin (2 μM, $n = 4$), or a β-receptor antagonist, propranolol (4 μM, $n = 5$), had no significant effect (Fig. 8*B*). As expected, an application of an α_2-agonist, clonidine (50 μM, $n = 6$), produced an outward current with a longer duration than NA (Fig. 8*C*). However an α_1-agonist, phenylephrine (50 μM, $n = 5$), or β-agonist, isoproterenol (50 μM, $n = 8$), showed no effect (data not shown). Figure 9 shows a summary of the suppressive effects of adrenergic antagonists (*A*) and agonists (*B*). The relative peak amplitude of the NA-induced outward current in the presence of an antagonist (*A*), and that of
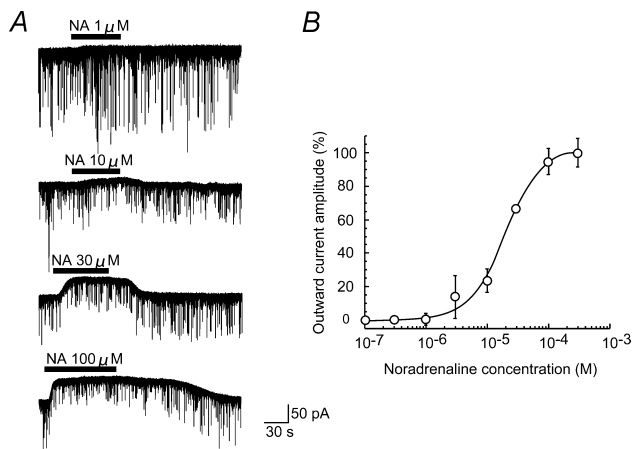
Figure 5. Dose dependency of outward current induced by NA

A, outward currents induced by NA at concentrations of 1, 10, 30 and 100 μM; these were obtained from the same neurone. *B*, normalized amplitude of outward current induced by NA was plotted against the NA concentration. Vertical bar indicates S.E.M. ($n = 3$–8). The continuous curve was drawn according to modified Michaelis–Menten equation with an EC$_{50}$ value of 20.5 μM. $V_H = -70$ mV.
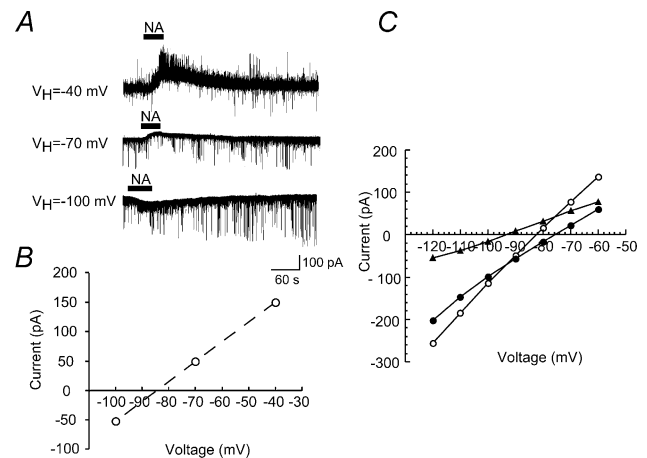
Figure 6. Voltage dependency of NA-induced current

A, NA (50 μM)-induced currents recorded at different V_H (−40, −70, −100 mV); these were obtained from the same neurone. *B*, amplitude of the membrane currents shown in *A* was plotted against V_H. *C*, amplitude of membrane currents in response to voltage pulses having a duration of 200 ms from $V_H = -70$ mV was plotted against voltages in the absence (filled circles) and presence (open circles) of NA (50 μM). The current–voltage relationship for net NA current was estimated from the difference between the current responses in the absence and presence of NA (filled triangles).

A

Cs$^+$

50 pA

10 s

B

GDP-β-S

50 pA

30 s
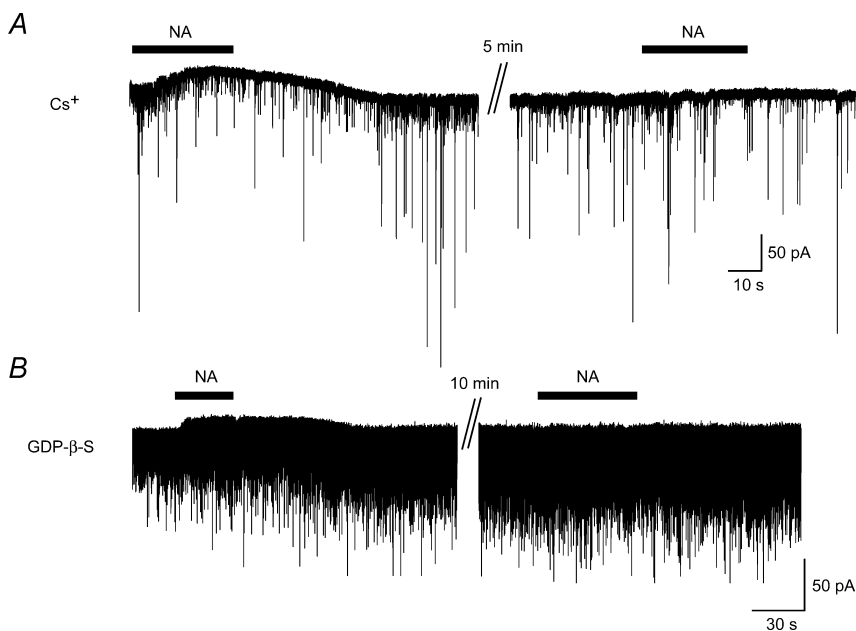
**Figure 7. Inhibition of NA-induced current by Cs and GDP-β-S**

A, outward current was recorded with Cs$^+$-containing pipette. NA induced an outward current just after establishing whole-cell recording. When NA was again applied 5 min later, the current was abolished. *B*, outward current was recorded with potassium gluconate pipette solution containing GDP-β-S. NA produced an outward current just after establishing whole-cell recording, but it was abolished when NA was again applied 10 min later.

the agonist-induced outward current (*B*) were expressed as a percentage of the peak amplitude induced by NA alone. These results suggest that the NA-induced outward current is mediated mainly by α_2-adrenoceptors.

Discussion

In the present study, the effects of NA on SG neurones were tested using the *in vivo* patch-clamp recording technique that enabled us to examine the effect of drugs on synaptic responses evoked by natural stimuli applied to

the skin. Previously we analysed the synaptic responses evoked by natural mechanical stimuli using the same technique, in which artificial ventilation together with bilateral pneumothorax was made to reduce a movement of spinal cord by respiration (Furue *et al.* 1999; Narikawa *et al.* 2000). However, in the present study we could maintain rats in good condition for more than 10 h and obtain stable patch-clamp recordings from SG neurones for up to 5 h without artificial ventilation. This method eliminated the operative stress for the animals produced by tracheal intubation and pneumothorax (Kehlet, 1991;

A

50 pA

30 s

B

50 pA

30 s

C

50 pA

30 s
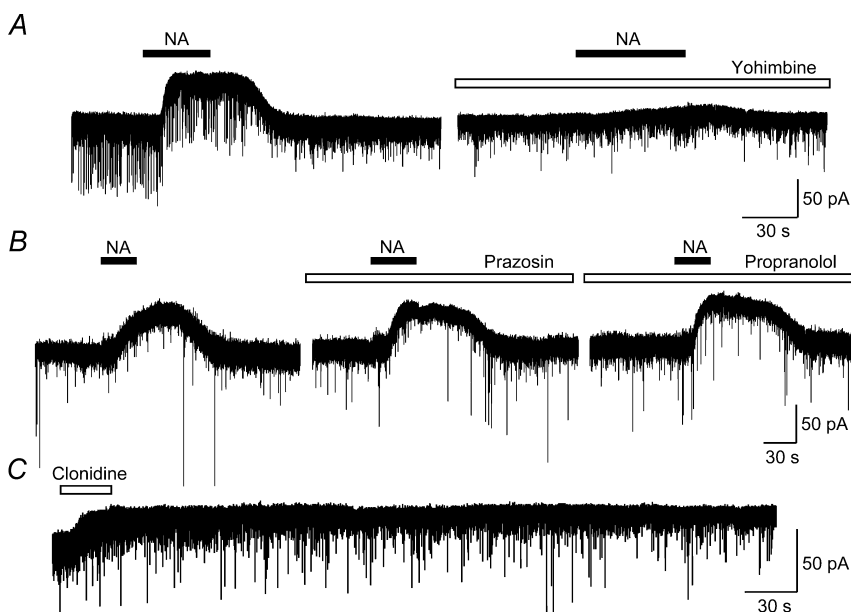
Figure 8. Effects of α_1-, α_2- and β-adrenergic antagonists and agonists

A, outward currents induced by NA (50 μM) were suppressed by simultaneous application of an α_2-antagonist, yohimbine (4 μM). *B*, an α_1-antagonist, prazosin (2 μM), and a β-antagonist, propranolol (4 μM), did not affect the amplitude of the NA-induced outward current. These were obtained from the same neurone. *C*, an α_2-agonist, clonidine (50 μM), produced an outward current as NA did, but showed a longer duration.

Kimmel & Still, 1999), as well as the time for preparing the artificial ventilation, which is a traditional technique of *in vivo* intracellular recordings.

There are several reports examining the effects of NA on neurones in the dorsal horn of the spinal cord to elucidate mechanisms of inhibition of nociceptive transmission by the descending inhibitory pathway. However, there have been no pharmacological studies using agonists and antagonists for adrenoceptor subtypes in whole-cell patch-clamp recordings under *in vivo* conditions. We applied drugs by perfusion on the surface of the spinal cord. If the amplitude and onset to peak of the NA-induced responses were to change depending on depth of the recorded neurones, it would be difficult to evaluate the rate of NA responsiveness and effects of agonists and antagonists on SG neurones that were located within a range from 50 to 150 μm. However, as shown in Fig. 4*B* and *C*, there was no clear correlation between amplitude and depth, and onset to peak and depth, suggesting that drugs perfused at the surface of the spinal cord and those administered by bath application in slice preparations acted equally on SG neurones. In addition, it was evident that the effects of NA were not mediated by systemic circulation since blood pressure or heart rate was not affected by NA. It is thus feasible to perform pharmacological investigations including determining the dose–response curve and the study of agonists or antagonists using the present drug application method.

In the present study, the pinch-evoked action potentials were substantially suppressed by the application of NA, probably due to the hyperpolarization of membrane potentials (Fig. 2*A*). However, in the voltage-clamp mode the pinch-induced EPSCs were markedly attenuated in amplitude by the application of NA (Fig. 2*B*). This depressive effect of NA was well preserved after blocking the postsynaptic action of NA by injection of Cs^+ and GDP-β-S, suggesting an involvement of presynaptic action of NA. Unexpectedly, NA has no significant effect on the frequency of miniature EPSCs in the presence of TTX, in spite of the fact that NA depresses the afferent evoked EPSCs after blockade of postsynaptic action. A possible explanation for this discrepancy is that SG neurones receive miniature inputs predominantly from interneurones and some from primary afferents. Assuming that NA receptors are expressed only at the primary afferent fibres, it would be reasonable that NA could depress the afferent-evoked EPSCs without affecting the mEPSCs. Alternatively, it is also conceivable that NA acts at a different process of the transmitter release mechanism, for instance calcium entry through N-, P- or Q-type channels, whereas, the mechanism for a miniature release is distinct from the evoked one. As shown in Fig. 3*B* and *D*, spontaneous EPSCs are observed in a substantial number of SG neurones *in vivo*, while spontaneous EPSCs are hardly recorded in slice preparations (Yoshimura & Nishi, 1993). Both the frequency and amplitude of spontaneous
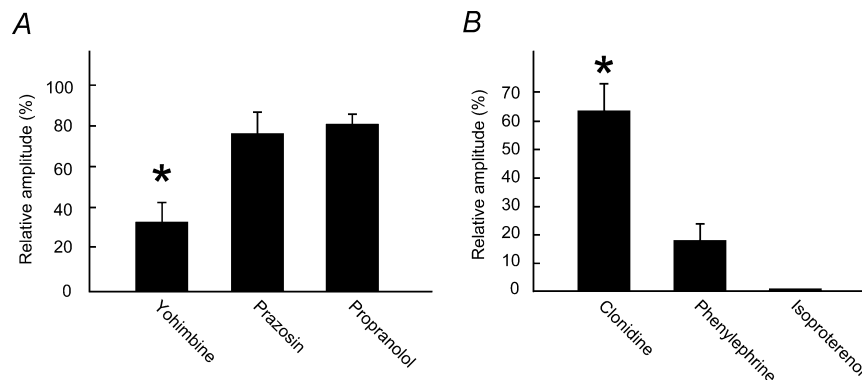
Figure 9. Summary of adrenergic antagonists and agonists
Relative peak amplitude (%) was calculated as an amplitude of NA (50 μM)-induced current in the presence of antagonist (*A*) or that of agonist-induced current (*B*) divided by that of currents produced by NA (50 μM) alone. *A*, NA (50 μM)-induced outward current in the presence of an α_2-receptor antagonist, yohimbine (4 μM, $n = 6$), was significantly smaller than that in the presence of an α_1-antagonist, prazosin (2 μM, $n = 4$), and a β-antagonist, propranolol (4 μM, $n = 5$) ($P < 0.01$, one-way ANOVA, yohimbine *versus* prazosin; $P < 0.05$, yohimbine *versus* propranolol; $P < 0.05$, prazosin *versus* propranolol; $P > 0.05$, Scheffe's *post hoc* test). *B*, relative amplitude of α_2-agonist clonidine (50 μM, $n = 6$)-induced outward current was significantly larger than that of α_1-agonist phenylephrine (50 μM, $n = 5$), and β-agonist isoproterenol (50 μM, $n = 8$)-induced currents ($P < 0.01$, one-way ANOVA clonidine *versus* phenylephrine; $P < 0.01$, clonidine *versus* isoproterenol; $P < 0.01$, phenylephrine *versus* isoproterenol; $P > 0.05$, Scheffe's test).

EPSCs observed in *in vivo* preparations are markedly depressed by NA as seen in Fig. 3*B*. This may be due to the membrane hyperpolarization in interneurones or presynaptic depression of transmitter release by NA acting at the terminals of the primary afferents. These findings are compatible with those of our previous study showing that bath application of NA decreased amplitude of Aδ fibre-/C fibre-mediated EPSCs under the condition of blockade of postsynaptic actions of NA by injection of Cs^+ and GDP-β-S, but not mEPSCs, of SG neurones in the spinal cord slices through α_2-adrenoceptors (Kawasaki *et al.* 2003). It has been also shown that α_{2A}-adrenoceptors are localized on the primary afferent terminals in the superficial layers of the dorsal horn of the spinal cord (Stone *et al.* 1998). The NA-induced blockade of noxious transmission is thus suggested to at least partly be mediated by the actions of NA on the presynaptic site to suppress the evoked EPSCs, thereby reducing the number of action potentials during pinching in SG neurones.

The application of NA induced outward currents or hyperpolarization in 85% of SG neurones in the present study as observed in *in vitro* studies (North & Yoshimura, 1984; Yajiri *et al.* 1997; Baba *et al.* 2000*a*,*b*). Since the NA-induced outward current is observed in the presence of TTX (Fig. 3*D*), it is suggested that NA has not only presynaptic but also postsynaptic actions to inhibit synaptic transmission in SG neurones. The NA-induced outward currents showed a reversal potential of −88 mV (Fig. 6), and were blocked by Cs^+ and GDP-β-S in pipette solution (Fig. 7). Furthermore, the outward currents were mimicked by an α_2-agonist, clonidine, and inhibited by an α_2-antagonist, yohimbine (Figs 8 and 9). These findings suggest that the NA-induced outward current is mediated by G-protein-activated K^+ channels through α_2-adrenoceptors. Our previous studies partly demonstrated the same results using intracellular (North & Yoshimura, 1984) and blind patch-clamp recordings (Yajiri *et al.* 1997) in slice preparations. Although we did not further examine the subtypes of α_2-adrenoceptors responsible for the NA-induced outward current, it was not blocked by prazosin in the present study (Figs 8 and 9). Since prazosin blocks not only α_1-adrenoceptors but also α_{2B}- and α_{2C}-adrenoceptors (Bylund *et al.* 1994), the effects of NA might be mediated by α_{2A}-adrenoceptors. Nevertheless, it has been shown that the majority of α_{2A}-adrenoceptors are localized on primary afferent fibres, while α_{2C}-adrenoceptors are expressed on spinal dorsal horn neurones (Stone *et al.* 1998; Olave & Maxwell, 2003*a*,*b*). The discrepancy between the anatomical and electrophysiological studies remains to be clarified.

The NA-induced outward currents and/or hyperpolarization induced by α_2-adrenergic receptor-mediated activation of K^+ channels have been reported in various neurones other than SG neurones, such as mesopontine cholinergic neurones (Williams & Reiner, 1993), median preoptic neurones (Bai & Renaud, 1998), and lateral septum neurones (Liu & Alreja, 1998) in slice preparations, and acutely dissociated locus ceruleus neurones (Arima *et al.* 1998). The ratio of the NA-sensitive neurones was high (70–90%) in those studies, similar to the present study (85%). They demonstrated that the K^+ channels activated by NA were inwardly rectifying (Williams & Reiner, 1993; Liu & Alreja, 1998; Bai & Renaud, 1998; Arima *et al.* 1998), but the same characteristic was not clearly demonstrated under *in vivo* conditions in the present study (Fig. 6*C*). In contrast, a small percentage of the neurones responded to NA with membrane depolarization in septal (Liu & Alreja, 1998) and median preoptic (Bai & Renaud, 1998) neurones, while we observed the inward currents in 2 out of 74 neurones. Although we did not further investigate the inward current, Bai & Renaud (1998) have shown that the depolarization was mediated by α_1-adrenoceptors.

One may consider that the EC_{50} of the NA-induced outward current (20 μM) is too high to evaluate the physiological roles of NA under *in vivo* conditions. However, an *in vivo* microdialysis study has shown that the electrical stimulation of descending noradrenergic fibres causes an increase in NA levels in the spinal cord up to 175.3 pmol per 20 min sampling time (Abhold & Bowker, 1990). Since the flow rate of the infusion pump was 2.13 μl min^{-1} and the recovery rate of the dialysis probe was about 18% in their study, the extracellular concentration of NA in the spinal cord was calculated to be about 23 μM. Therefore, the concentration used in the present study is considered to correspond to the increased NA levels induced by the activation of the descending noradrenergic pathway. In slice experiments, IC_{50} (an inhibition to a near-maximal effect of NA (100 μM)) was 17.7 μM (Liu & Alreja, 1998), while in dissociated neurones EC_{50} was 220 nM (Arima *et al.* 1998), suggesting that the enzymatic degradation of NA could affect the EC_{50} significantly in the slice and *in vivo* experiments.

In conclusion, the present study using the *in vivo* patch-clamp technique suggested that the antinociceptive effects of NA originating from the descending noradrenergic pathway are mediated by the actions on both (1) presynaptic sites thereby reducing noxious stimuli-induced EPSCs and (2) postsynaptic SG neurones inducing hyperpolarizations by interacting with α_2-adrenoceptor- and G-protein-mediated activation of K^+ channels. In

addition to these actions, we have previously shown that NA enhances miniature and spontaneous IPSCs in SG neurones by activating GABAergic and/or glycinergic interneurones, which are present in the SG (Todd & McKenzie, 1989), through α_1-adrenoceptors (Baba *et al.* 2000*a,b*). Our *in vivo* patch-clamp experiments in rats demonstrated that cutaneous mechanical stimulation including brushing evokes both EPSCs (Furue *et al.* 1999) and IPSCs (Narikawa *et al.* 2000) in SG neurones. Further investigations will thus be required to test the effects of NA and/or stimulation of the descending noradrenergic pathway on EPSCs and IPSCs produced by touch as well as pinch stimuli under *in vivo* patch-clamp conditions.

References

Abhold RH & Bowker RM (1990). Descending modulation of dorsal horn biogenic amines as determined by in vivo dialysis. *Neurosci Lett* **108**, 231–236.

Arima J, Kubo C, Ishibashi H & Akaike N (1998). α2-Adrenoceptor-mediated potassium currents in acutely dissociated rat locus coeruleus neurones. *J Physiol* **508**, 57–66.

Baba H, Goldstein PA, Okamoto M, Kohno T, Ataka T, Yoshimura M & Shimoji K (2000*a*). Norepinephrine facilitates inhibitory transmission in substantia gelatinosa of adult rat spinal cord (part 2): effects on somatodendritic sites of GABAergic neurons. *Anesthesiology* **92**, 485–492.

Baba H, Shimoji K & Yoshimura M (2000*b*). Norepinephrine facilitates inhibitory transmission in substantia gelatinosa of adult rat spinal cord (part 1): effects on axon terminals of GABAergic and glycinergic neurons. *Anesthesiology* **92**, 473–484.

Bai D & Renaud LP (1998). Median preoptic nucleus neurons: an in vitro patch-clamp analysis of their intrinsic properties and noradrenergic receptors in the rat. *Neuroscience* **83**, 905–916.

Beal JA & Bicknell HR Jr (1985). Development and maturation of neurons in the substantia gelatinosa (SG) of the rat spinal cord. In *Development, Organization and Processing in Somatosensory Pathways*, ed. Rowe M & Willis WD Jr, pp. 23–30. Wiley-Liss, New York.

Bylund DB, Eikenberg DC, Hieble JP, Langer SZ, Lefkowitz RJ, Minneman KP, Molinoff PB, Ruffolo RR Jr & Trendelenburg U (1994). International Union of Pharmacology nomenclature of adrenoceptors. *Pharmacol Rev* **46**, 121–136.

Concepcion M, Maddi R, Francis D, Rocco AG, Murray E & Covino BG (1984). Vasoconstrictors in spinal anesthesia with tetracaine – a comparison of epinephrine and phenylephrine. *Anesth Analg* **63**, 134–138.

Fairbanks CA, Stone LS, Kitto KF, Nguyen HO, Posthumus IJ & Wilcox GL (2002). α_{2C}-Adrenergic receptors mediate spinal analgesia and adrenergic-opioid synergy. *J Pharmacol Exp Ther* **300**, 282–290.

Furue H, Narikawa K, Kumamoto E & Yoshimura M (1999). Responsiveness of rat substantia gelatinosa neurones to mechanical but not thermal stimuli revealed by in vivo patch-clamp recording. *J Physiol* **521**, 529–535.

Hagihira S, Senba E, Yoshida S, Tohyama M & Yoshiya I (1990). Fine structure of noradrenergic terminals and their synapses in the rat spinal dorsal horn: an immunohistochemical study. *Brain Res* **526**, 73–80.

Headley PM, Duggan AW & Griersmith BT (1978). Selective reduction by noradrenaline and 5-hydroxytryptamine of nociceptive responses of cat dorsal horn neurones. *Brain Res* **145**, 185–189.

Howe JR, Wang JY & Yaksh TL (1983). Selective antagonism of the antinociceptive effect of intrathecally applied alpha adrenergic agonists by intrathecal prazosin and intrathecal yohimbine. *J Pharmacol Exp Ther* **224**, 552–558.

Howe JR & Zieglgansberger W (1987). Response of rat dorsal horn neurons to natural stimulation and to iontophoretically applied norepinephrine. *J Comp Neurol* **255**, 1–17.

Kasai M & Mizumura K (2001). Increase in spontaneous action potentials and sensitivity in response to norepinephrine in dorsal root ganglion neurons of adjuvant inflamed rats. *Neurosci Res* **39**, 109–113.

Kawasaki Y, Kumamoto E, Furue H & Yoshimura M (2003). Alpha 2 adrenoceptor-mediated presynaptic inhibition of primary afferent glutamatergic transmission in rat substantia gelatinosa neurons. *Anesthesiology* **98**, 682–689.

Kehlet H (1991). The surgical stress response: should it be prevented? *Can J Surg* **34**, 565–567.

Kimmel EC & Still KR (1999). Acute lung injury, acute respiratory distress syndrome and inhalation injury: an overview. *Drug Chem Toxicol* **22**, 91–128.

Kumazawa T & Perl ER (1978). Excitation of marginal and substantia gelatinosa neurons in the primate spinal cord: indications of their place in dorsal horn functional organization. *J Comp Neurol* **177**, 417–434.

Liu W & Alreja M (1998). Norepinephrine inhibits neurons of the intermediate subnucleus of the lateral septum via alpha2-adrenoceptors. *Brain Res* **806**, 36–54.

McLachlan EM, Janig W, Devor M & Michaelis M (1993). Peripheral nerve injury triggers noradrenergic sprouting within dorsal root ganglia. *Nature* **363**, 543–546.

Narikawa K, Furue H, Kumamoto E & Yoshimura M (2000). In vivo patch-clamp analysis of IPSCs evoked in rat substantia gelatinosa neurons by cutaneous mechanical stimulation. *J Neurophysiol* **84**, 2171–2174.

North RA & Yoshimura M (1984). The actions of noradrenaline on neurons of the rat substantia gelatinosa in vitro. *J Physiol* **349**, 43–55.

Olave MJ & Maxwell DJ (2003*a*). Neurokinin-1 projection cells in the dorsal horn receive synaptic contents from axons that possess α_{2C}-adrenergic receptors. *J Neurosci* **23**, 6837–6846.

Olave MJ & Maxwell DJ (2003*b*). Axon terminals possessing the α_{2C}-adrenergic receptor in the rat dorsal horn are predominantly excitatory. *Brain Res* **965**, 269–273.

Perl ER (1999). Causalgia, pathological pain, and adrenergic receptors. *Proc Natl Acad Sci U S A* **96**, 7664–7667.

Petersen CCH, Grinvald A & Sakmann B (2003). Spatiotemporal dynamics of sensory responses in layer 2/3 of rat barrel cortex measured in vivo by voltage-sensitive dye imaging combined with whole-cell voltage recordings and neuron reconstructions. *J Neurosci* **23**, 1298–1309.

Rajaofetra N, Ridet JL, Poulat P, Marlier L, Sandillon F, Geffard M & Privat A (1992). Immunocytochemical mapping of noradrenergic projections to the rat spinal cord with an antiserum against noradrenaline. *J Neurocytol* **21**, 481–494.

Reddy SV, Maderdrut JL & Yaksh TL (1980). Spinal cord pharmacology of adrenergic agonist-mediated antinociception. *J Pharmacol Exp Ther* **213**, 525–533.

Rexed B (1952). The cytoarchitectonic organization of the spinal cord in the cat. *J Comp Neurol* **96**, 415–495.

Satoh K, Kashiba A, Kimura H & Maeda T (1982). Noradrenergic axon terminals in the substantia gelatinosa of the rat spinal cord: an electron-microscopic study using glyoxylic acid-potassium permanganate fixation. *Cell Tissue Res* **222**, 359–378.

Spike RC & Todd AJ (1992). Ultrastructural and immunocytochemical study of lamina II islet cells in rat spinal dorsal horn. *J Comp Neurol* **323**, 359–369.

Stone LS, Broberger C, Vulchanova L, Wilcox GL, Hokfelt T, Riedl MS & Elde R (1998). Differential distribution of α_{2A} and α_{2C} adrenergic receptor immunoreactivity in the rat spinal cord. *J Neurosci* **18**, 5928–5937.

Stone LS, MacMillan LB, Kitto KF, Limbird LE & Wilcox GL (1997). The α_{2A} adrenergic receptors subtype mediates spinal analgesia evoked by α2 agonists and is necessary for spinal adrenergic-opioid synergy. *J Neurosci* **17**, 7157–7165.

Sugiura Y, Lee CL & Perl ER (1986). Central projection of identified, unmyelinated (C) afferent fibers innervating mammalian skin. *Science* **234**, 358–361.

Todd AJ & McKenzie J (1989). GABA-immunoreactive neurons in the dorsal horn of the rat spinal cord. *Neuroscience* **31**, 799–806.

Vaida GT, Moss P, Capan LM & Turndorf H (1986). Prolongation of lidocaine spinal anesthesia with phenylephrine. *Anesth Analg* 65, 781–785.

Westlund KN, Bowker RM, Ziegler MG & Coulter JD (1982). Descending noradrenergic projections and their spinal terminations. *Prog Brain Res* **57**, 219–238.

Williams JA & Reiner PB (1993). Noradrenaline hyperpolarizes identified rat mesopontine cholinergic neurons in vivo. *J Neurosci* **13**, 3878–3883.

Woolf CJ & Fitzgerald M (1983). The properties of neurones recorded in the superficial dorsal horn of the rat spinal cord. *J Comp Neurol* **221**, 313–328.

Yajiri Y, Yoshimura M, Okamoto M, Takahashi H & Higashi H (1997). A novel slow excitatory postsynaptic current in substantia gelatinosa neurons of the rat spinal cord in vitro. *Neuroscience* **76**, 673–688.

Yoshimura M & Jessell TM (1989). Primary afferent-evoked synaptic responses and slow potential generation in rat substantia gelatinosa neurons in vitro. *J Neurophysiol* **62**, 96–108.

Yoshimura M & Nishi S (1993). Blind patch-clamp recordings from substantia gelatinosa neurons in adult rat spinal cord slices: pharmacological properties of synaptic currents. *Neuroscience* **53**, 519–526.

Zang LI, Tan AY, Schreiner CE & Merzenich MM (2003). Topography and synaptic shaping of direction selectivity in primary auditory cortex. *Nature* **424**, 201–205.

Acknowledgements